Title

Requirement for kasB in Mycobacterium mycolic acid biosynthesis, cell wall impermeability and intracellular survival: implications for therapy

Journal

Molecular Microbiology, 49(6)

ISSN

0950-382X

Authors

Gao, L Y
Laval, F
Lawson, E H
et al.

Publication Date

2003-09-01

Peer reviewed

Molecular Microbiology (2003) **49**(6), 1547–1563 doi:10.1046/j.1365-2958.2003.03667.x

Requirement for *kasB* in *Mycobacterium* mycolic acid biosynthesis, cell wall impermeability and intracellular survival: implications for therapy

Lian-Yong Gao,[1] Francoise Laval,[2] Elise H. Lawson,[1] Richard K. Groger,[3] Andy Woodruff,[1] J. Hiroshi Morisaki,[1] Jeffery S. Cox,[1,4] Mamadou Daffe[2] and Eric J. Brown[1]*

[1]*Program in Host-Pathogen Interactions, UCSF Campus Box 2140, 600 16th St, San Francisco, CA 94143–2140, USA.*

[2]*Department of Molecular Mechanisms of Mycobacterial Infections, Institut of Pharmacologie et Biologie structurale, (UMR 5089), Toulouse, France.*

[3]*Department of Medicine, Washington University School of Medicine, St Louis, MO 63110, USA.*

[4]*Department of Microbiology and Immunology, University of California San Francisco, CA 94143, USA.*

Summary

Mycobacterium tuberculosis **infects one-third of the world's population and causes two million deaths annually. The unusually low permeability of its cell wall contributes to the ability of *M. tuberculosis* to grow within host macrophages, a property required for pathogenesis of infection. *Mycobacterium marinum* is an established model for discovering genes involved in mycobacterial infection. *Mycobacterium marinum* mutants with transposon insertions in the β-ketoacyl-acyl carrier protein synthase B gene (*kasB*) grew poorly in macrophages, although growth *in vitro* was unaffected. Detailed analyses by thin-layer chromatography, nuclear magnetic resonance (NMR), matrix-assisted laser desorption/ionization time-of-flight mass spectrometry, infrared spectroscopy, and chemical degradations showed that the *kasB* mutants synthesize mycolic acids that are 2–4 carbons shorter than wild type; the defect was localized to the proximal portion of the meromycolate chain. In addition, these mutants showed a significant (~30%) reduction in the abundance of keto-mycolates, with a slight compensatory increase of both α- and methoxy-mycolates. Despite these small changes in mycolate length and composition, the *kasB* mutants exhibited strikingly altered cell wall permeability, leading to a marked increase in susceptibility to lipophilic antibiotics and the host antimicrobial molecules defensin and lysozyme. The abnormalities of the *kasB* mutants were fully complemented by expressing *M. tuberculosis kasB*, but not by the closely related gene *kasA*. These studies identify *kasB* as a novel target for therapeutic intervention in mycobacterial diseases.**

Accepted 10 June, 2003. *For correspondence. E-mail ebrown@medicine.ucsf.edu; Tel. (+1) 415 514 0167; Fax (+1) 415 514 0169.

Introduction

The global burden of *Mycobacterium tuberculosis* infection is overwhelming, with approximately one-third of the world's population infected and two million deaths each year (Dolin *et al*., 1994). High rates of disease and death from *M. tuberculosis* infection are primarily due to the bacterium's extreme infectivity and its ability to persist intracellularly and in other sites of the host poorly accessible to antibiotics. Resistance to commonly used antibiotics also has emerged as an increasing problem for control of the global epidemic. *Mycobacterium tuberculosis* has evolved sophisticated strategies to combat host defence mechanisms through co-evolution with humans and can modulate a number of host cell processes to benefit its intracellular parasitism (Gao and Kwaik, 2000; Russell, 2001). It also possesses a cell wall of unusually low permeability that resists an array of host defence mechanisms and chemotherapeutic agents (Brennan and Nikaido, 1995; Barry *et al*., 1998; Daffe and Draper, 1998; Jarlier and Nikaido, 1994). The primary constituents of this low–permeability barrier are mycolic acids (very long-chain fatty acids) that esterify either to cell wall arabinogalactan, leading to a continuous link with peptidoglycan, or to trehalose to yield a pool non-covalently associated with the outer layer of the cell envelope (Brennan and Nikaido, 1995; Barry *et al*., 1998; Daffe and Draper, 1998; Liu and Nikaido, 1999). It is apparent that a detailed understanding of the structure and function of mycolic acids and their biosynthetic pathway should lead to discovery of novel targets for the design of potent antimycobacterial drugs.

The structures of mycolic acids of several mycobacterial species have been determined using combinations of the

technologies of thin layer chromatography (TLC), mass spectrometry (MS), nuclear magnetic resonance (NMR), and infrared spectroscopy (IR). The general structure of mycolic acids is R-CH(OH)-CH(R′)-COOH, where R is a 'meromycolate' chain (mero-chain) consisting of 50–60 carbons and R′ is a shorter aliphatic chain (α-branch) possessing 22–26 carbons. Structural variations in the functional groups of the mero-chain are used to classify mycolic acids into major groups, each of which shows microheterogeneity in carbon chain lengths. *Mycobacterium tuberculosis* produces three distinct mycolate groups: α-, methoxy-, and keto-mycolates (Fig. 1). α-mycolates contain two *cis*-cyclopropane rings, whereas in methoxy- and keto-mycolates the distal cyclopropane is replaced by a carbon-oxygen bond with an adjacent methyl branch, and the proximal cyclopropane has either a *cis* or *trans* configuration (Brennan and Nikaido, 1995; Barry *et al*., 1998; Daffe and Draper, 1998). These modifications of the mero-chain are introduced by a family of methyl-transferases (Dubnau *et al*., 2000; Glickman *et al*., 2001). A growing body of evidence suggests that these modifications play an important role in mycobacterial cell wall impermeability, cording, and virulence. For example, cyclopropanation of α-mycolates at the distal position enhances resistance of *Mycobacterium smegmatis* to oxidative killing (Yuan *et al*., 1995), whereas this modification at the proximal function enhances cell wall impermeability of *M. smegmatis* (George *et al*. 1995), as well as cording and persistence of *M. tuberculosis* in mouse tissues (Glickman *et al*., 2000). Similarly, oxygenation of mycolates (methoxy and keto) enhances the ability of *M. tuberculosis* to infect mice and cells (Yuan *et al*., 1998; Dubnau *et al*., 2000). In addition, markedly increased production of keto-mycolates has been observed for *M. tuberculosis* and *Mycobacterium microti* growing inside mouse macrophages (Yuan *et al*., 1998) and lung tissues (Davidson *et al*., 1982), suggesting the importance of this species of mycolates for bacterial survival during infection. How mycolate composition affects cell wall function is not understood, but a *M. smegmatis* mutant that accumulates incomplete meromycolate chains instead of mycolic acids exhibits marked increases in cell wall permeability and thermodynamic fluidity (Liu and Nikaido, 1999).

The mechanism of elongation of mycolates is not well understood. The genome sequence of *M. tuberculosis* (Cole *et al*., 1998) has predicted the presence of two fatty acid synthase (FAS) systems, FAS-I (a multifunctional single polypeptide) and FAS-II (a multiple enzyme complex). Past studies examining accumulation of mycolate precursors (Qureshi *et al*., 1998) or *in vitro* β-ketoacyl-acyl carrier protein synthase (KAS) activities (Kremer *et al*., 2000; 2002; Schaeffer *et al*., 2001; Slayden and Barry, 2002) have suggested that FAS-I is involved in elongation of short-chain compounds to yield fatty acids of 16–26 carbons that are further extended to full lengths by FAS-II. Several putative FAS-II components are located in a gene cluster containing both *kasA* and *kasB* (Cole *et al*., 1998), the only two genes that encode enzymes that have been shown to possess FAS-II KAS activity *in vitro*. A previous study suggested that isoniazid (INH) inhibition of *M. tuberculosis* mycolate production might occur through formation of a complex with KasA (Mdluli *et al*., 1998). Recently, by using an *in vitro* fatty acid biosynthesis assay system, Schaeffer *et al*. (2001) and Kremer *et al*. (2002) showed that purified KasA or KasB of *M. tuberculosis* elongates fatty acids with substrate specificity of ≥14 carbons. Another recent study by Slayden and Barry (2002) showed that cell lysates of *M. smegmatis* expressing *M. tuberculosis kasA* could elongate fatty acids to ~40 carbons, whereas expression of

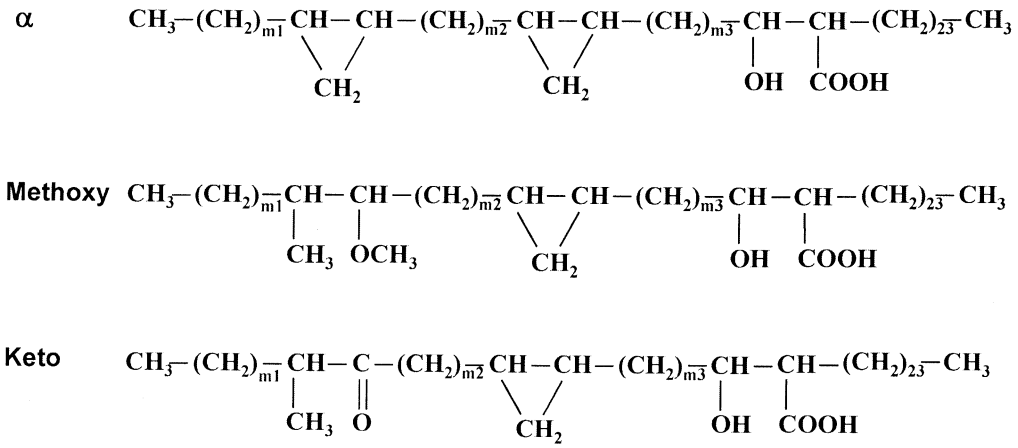

Fig. 1. Structures of the major mycolic acids of *M. tuberculosis* $H_{37}Rv$ (Laval *et al*., 2001). The main values of m_1 and m_3 are 15, 17, and 19; those of m_2 depend on the presence (13, 15, and 17) or absence (12, 14, and 16) of a methyl branch at the proximal location. Full length mycolates have 78 and 80 carbons for α; 83, 85, and 87 carbons for methoxy; and 84 and 86 carbons for keto.

both *kasA* and *kasB* produced longer chain fatty acids (~54 carbons) equivalent in length to the mero-chains of mycolates. Based on these *in vitro* biosynthesis and drug inhibition studies, it has been proposed that *kasA* is involved in the initial elongation of mycolates that are extended to their full lengths by *kasB* (Kremer *et al*., 2002; Slayden and Barry, 2002). However, direct *in vivo* tests of this hypothesis are lacking.

Mycobacterium marinum, a fish, amphibian and opportunistic human pathogen, has been developed recently as a model system for studying *M. tuberculosis* pathogenesis (Ramakrishnan *et al*., 1997; 2000; Talaat *et al*., 1998; Gao *et al*., 2003). *Mycobacterium marinum* is phylogenetically close to members of the *M. tuberculosis* complex (Tonjum *et al*., 1998), and the infection it causes in its natural hosts manifests pathological hallmarks of tuberculosis, including granulomas (Ramakrishnan *et al*., 1997; Talaat *et al*., 1998). These observations suggest that many of the basic mechanisms of disease initiation are conserved between *M. marinum* and *M. tuberculosis*. Furthermore, these two mycobacterial species have in common a number of lipids including phenolic glycolipids, phthiocerol diesters and mycolate profiles (Daffe and Draper, 1998). In addition, *M. marinum* grows significantly faster than *M. tuberculosis* and other slow-growing mycobacteria, with a generation time of 4 h, compared to 20 h for *M. tuberculosis*. Therefore, *M. marinum* offers an attractive and potentially valuable model for studying the molecular biology of mycobacterial pathogenesis. We have recently developed a highly efficient *mariner*-based transposon *m*utagenesis system in *M. marinum* (M4) for facile generation of random mutations and construction of a mutant library (Gao *et al*., 2003). This library has been used to identify mutants with distinct phenotypes potentially important for mycobacterial virulence. We recently reported identification of a *M. marinum* mutant attenuated for intracellular growth in macrophages that was fully complemented by a homologous *M. tuberculosis* locus (Gao *et al*., 2003). In the present work, we describe isolation of *M. marinum kasB* mutants and show that *kasB* is required for normal growth of *M. marinum* in macrophages. Whereas *kasB* is required for full elongation of mycolates to their mature forms, the defect in the lengths of the mycolates in these *kasB* mutants is rather small (~2–4 carbon units). Despite the small difference in mycolate length, the *kasB* mutants have markedly increased permeability of their cell walls and consequently are severely defective in resisting host defence mechanisms and antibiotic action. Complete recovery of the *kasB* mutants to wild-type phenotypes is achieved by ectopic expression of the *M. tuberculosis kasB* gene, but not by *kasA*. These studies identify *kasB* as an important potential target for novel therapeutic intervention, independent of *kasA*.

Results

Identification of M. marinum kasB *mutants with impaired growth within macrophages*

Our screen of a *M. marinum* transposon mutant library developed by the M^4 procedure has identified 24 mutants with impaired growth in J774 murine macrophage-like cells (our unpublished results). Sequencing of the transposon insertion junctions identified three mutants (4B8, 4E4 and 4E8) with independent insertions in a gene that is homologous to *M. tuberculosis kasB* (Fig. 2A) (Cole *et al*., 1998). Whereas the 4B8 and 4E8 mutants had transposon insertions that disrupted the coding sequence of *kasB*, the 4E4 mutant had a transposon insertion at the 3′ end of the gene, with a direction of transcription of the kanamycin-resistant gene (Kan^r) opposite to *kasB*. Based on both our sequencing data and the assembled contig (mar821d11.p1n) of the incomplete *M. marinum* genome database at the Sanger Center, KasB of *M. marinum* is 89% identical and 93% homologous to *M. tuberculosis* KasB. In addition, both the sequences and genomic organization of genes surrounding *kasB* are conserved between *M. marinum* and *M. tuberculosis*. *M. marinum* KasA shows even higher similarity to *M. tuberculosis* KasA, sharing 92% identity and 97% similarity.

The three *M. marinum kasB* mutants showed ~10-fold fewer CFUs compared to wild type for infection of J774 cells at 4 days after infection (Fig. 2B). These mutants also showed reduced intracellular growth in murine bone marrow-derived macrophages (MDMs) (Fig. 2C). Coincident with the decreased rate of intracellular growth was a decrease in host cell cytotoxicity of the infection, as the J774 monolayer was lysed by wild-type *M. marinum* at 4 days but not until ≥6 days by the mutants (data not shown). The intracellular growth defect of the *kasB* mutants was not due to a general metabolic abnormality of these bacterial strains, as they grew similarly to wild type in bacterial culture medium (Fig. 3A and data not shown). These results demonstrate that *kasB* is required for a normal growth rate of *M. marinum* during macrophage infection.

Complementation of M. marinum kasB *mutants by* M. tuberculosis kasB *gene*

The high degree of similarity between KasB of *M. marinum* and *M. tuberculosis* provided an opportunity to assess the utility of *M. marinum* as a model organism for studying the function of *M. tuberculosis* genes. We expressed the coding sequence of the *M. tuberculosis kasB* gene in each of the three *kasB* mutants and examined their growth in J774 cells. Expression of *M. tuberculosis kasB* fully restored intracellular growth of all three *kasB* mutants (Fig. 3B and data not shown). In addition,

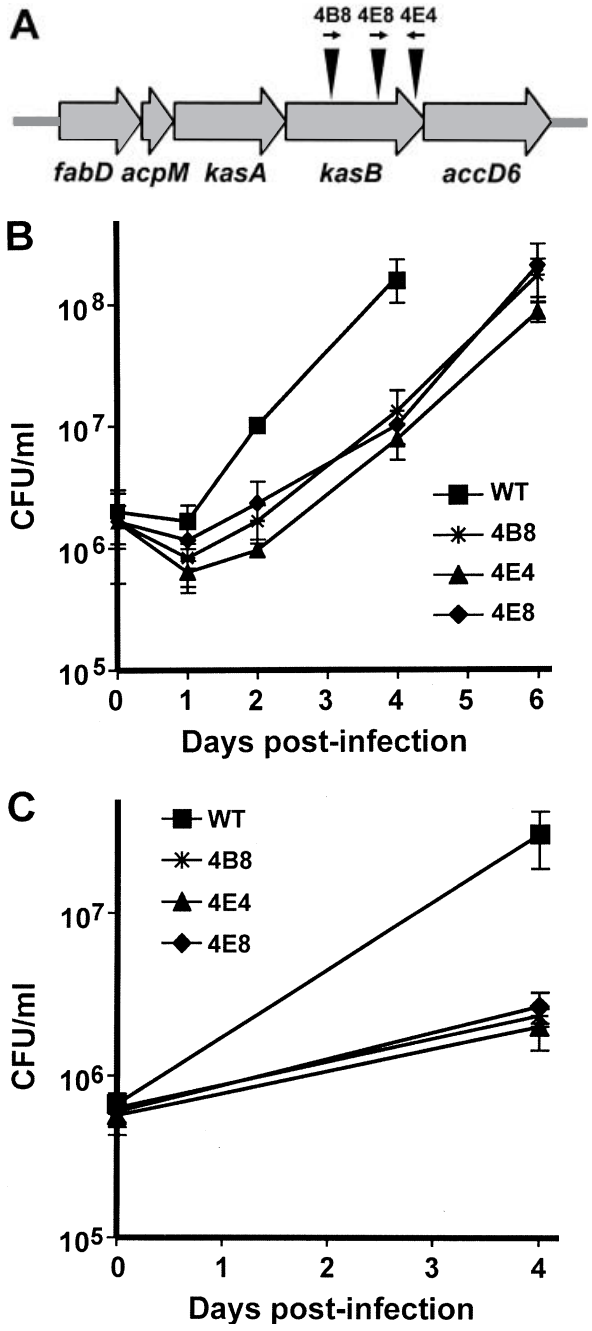

Fig. 2. A. Partial map of *M. marinum fasII* locus and transposon insertions (vertical triangles) in the *kasB* gene at different orientations (black arrows indicate the direction of the transcription of the Kan^r gene).
B and C. Growth kinetics of *M. marinum* wild type and the *kasB* mutants in J774 cells and MDMs respectively.

the kinetics of cytotoxicity was also restored to wild type (data not shown). Expression of the downstream gene *accD6* did not complement the *kasB* mutants, and co-expression of *kasB* and *accD6* had a phenotype indistinguishable from expression of *kasB* alone (data not shown). Therefore, the growth defect of these three mutants was due to mutation of *kasB* and not a polar effect on downstream genes. Given the high degree of similarity between KasB and KasA, we examined whether expression of *M. tuberculosis kasA* could complement the *kasB* defect. Surprisingly, our results showed that *M. tuberculosis kasA* exacerbated the growth defect of the 4B8 mutant (Fig. 3B). The worsened defect of the *kasA*-expressing strain might be due in part to generally decreased hardiness, as the transformed strain also grew less well *in vitro* (Fig. 3A). To determine whether this general toxicity of expression of *kasA* was specific to the *M. tuberculosis* gene, *M. marinum kasA* gene also was expressed in each of the *kasB* mutants, and similar effects were observed (data not shown). Together, these results demonstrate that *kasB* has a unique and non-redundant role required for normal growth of mycobacteria in macrophages.

Cell wall mycolates are shortened in kasB *mutants*

Previous characterization of *in vitro* activity of KasA and KasB and inhibition of mycolate biosynthesis by INH have led to the hypothesis that both enzymes are required for elongation of mycolates during bacterial growth. To examine the effect of *kasB* mutation on mycolate biosynthesis, we examined mycolate profiles of *M. marinum* strains by high performance TLC (HPTLC). There was no difference among these *M. marinum* strains in the amount of total mycolates or mycolic acids either covalently bound to or non-covalently associated with the cell wall, as determined by quantification of ^{14}C-acetate-labelled mycolates (data not shown). There was also no difference among these strains in the appearance and abundance of polar and apolar organic extractable cell wall lipids (data not shown). When separated by silica HPTLC plates, the mycolates of wild-type *M. marinum* showed three groups of mycolates (α, methoxy, and keto) (Fig. 4A), similar to those of *M. tuberculosis* (Dubnau *et al*., 2000) and in agreement with previous reports (Daffe *et al*., 1991; Chemlal *et al*., 2002). Although the 4B8 mutant had all three groups of the mycolates, the TLC mobility of each one was slightly but reproducibly reduced compared to wild type (Fig. 4A), suggesting the possibility of shortened carbon chain lengths. More prominent differences of migration were observed by reverse phase HPTLC for each of the three groups of mycolates isolated from wild type and the 4B8 mutant, under solvent conditions in which shorter chains run faster on the TLC plates (Fig. 4B). α-mycolates of wild-type *M. marinum* contained five major microheterogeneous species; in contrast, α-mycolates of the 4B8 mutant had only three major species equivalent to the three fastest migrating species of wild type (Fig. 4B). The

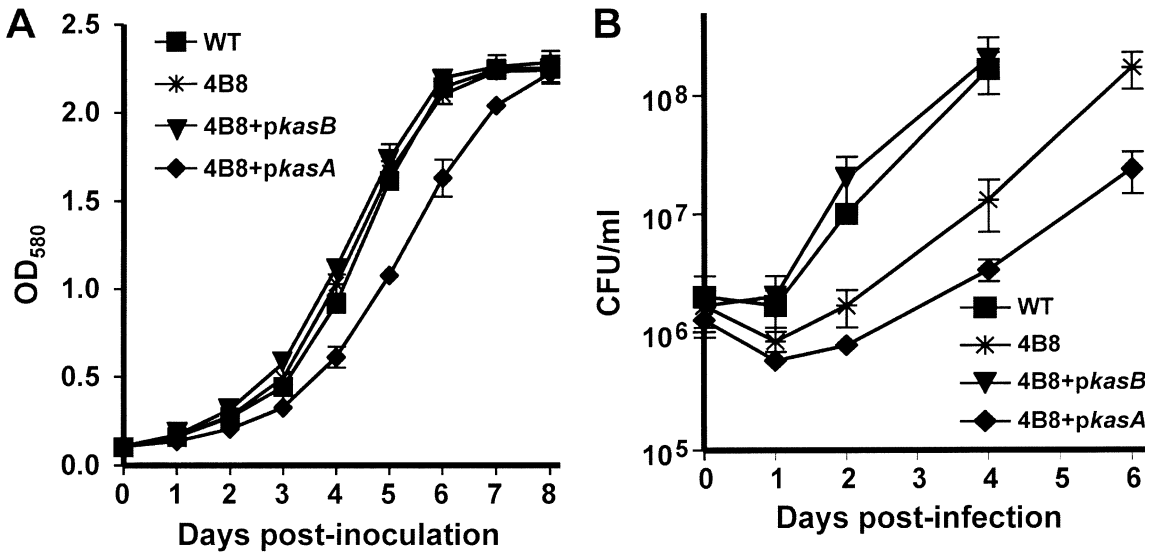

Fig. 3. Growth kinetic of *M. marinum* strains in 7H9 broth (A) or J774 cells (B). OD_{580}, optical density at the wavelength of 580 nm.

4B8 mutant likewise did not have the two slowest migrating species of the oxygenated mycolates (methoxy and keto) that were present in wild-type *M. marinum* (Fig. 4B). Whereas expression of *M. tuberculosis kasB* completely corrected these migration defects of the 4B8 mutant, expression of *kasA* did not.

In addition to these carbon chain length variations, there were differences in abundance of the three groups of mycolates between wild type and the *kasB* mutants. The percentage of α-, methoxy- or keto-mycolates in total mycolates for wild type was 41, 24 and 35% respectively (Fig. 4C). The 4B8 mutant showed a significant (~30%) reduction in the abundance of keto-mycolates, with a slight compensatory increase of both α- and methoxy-mycolates. Complementation with *M. tuberculosis kasB*, but not *kasA*, corrected this abnormality in the relative abundance of these mycolate species.

To confirm shortened mycolates in the *kasB* mutant as suggested by TLC, mycolates from strains of *M. marinum* were analysed by matrix-assisted laser desorption/ionization time-of-flight mass spectrometry (MALDI-TOF MS). Mass spectra matched well with the mycolate profiles revealed by HPTLC, demonstrating that the predominant chain lengths were 2–4 carbons shorter for oxygenated mycolates in the absence of *kasB* (Fig. 5 and Table 1). Oxygenated mycolates of wild type had chain lengths corresponding to 79–85 carbons (methoxy) and 80–82 carbons (keto), as opposed to 77–81 and 76–80 carbons, respectively, in the mutant (Fig. 5 and Table 1). Similarly, whereas α-mycolates of wild type had 73–80 carbons, those of the 4B8 mutant had 73–76 carbons (Table 1) (Laval *et al.*, 2001). As already seen in other assays of complementation, *M. tuberculosis kasB*, but not *kasA*, reverted the mycolate length differences in the mutant to wild-type sizes.

Detailed analysis of mycolates

Further analysis by NMR, IR and argentation TLC demonstrated that the global structures of the three types of mycolates from wild type and *kasB* mutants were similar. α-mycolates consisted primarily of dicyclopropanated compounds (IR bands at 1020 and 3060 cm^{-1}). The *cis* configuration of cyclopropyl groups in the α-mycolates was established by ^{1}H-NMR analysis (signals at – 0.3, 0.6 and 0.7 p.p.m.). Minor *cis* (^{1}H-NMR signals at 5.35 p.p.m) and *trans* (IR bands at 970 cm^{-1} and ^{1}H-NMR signals at 5.25 p.p.m.) ethylenic α-mycolates also occurred in both strains. In contrast to *M. tuberculosis*, the oxygenated mycolates of wild-type and 4B8 mutant *M. marinum* were composed almost exclusively of ethylenic forms, consistent with published data (Daffe *et al.*, 1991); the configuration of the double bond was predominantly *trans* in both methoxy- and keto-mycolates (IR bands at 970 cm^{-1}; ^{1}H-NMR signals at 5.25 p.p.m.) with an adjacent methyl branch (^{1}H-NMR doublets at 0.94 p.p.m.), although the presence of ethylenic oxygenated mycolates with a *cis* configuration (^{1}H-NMR signals at 5.35 p.p.m.) was also detected.

To investigate the location of the 2–4 carbons in wild-type mycolates missing from the *kasB* mutants, mycolates purified from wild type and 4B8 were analysed by chemical degradation methods. Pyrolysis of the individual types of mycolates, a reaction that occurs during GC and GC-MS analyses of mycolates and cleaves the molecules into α-branches and mero-chains, showed that α-branches of the mycolates from both wild type and mutant contained

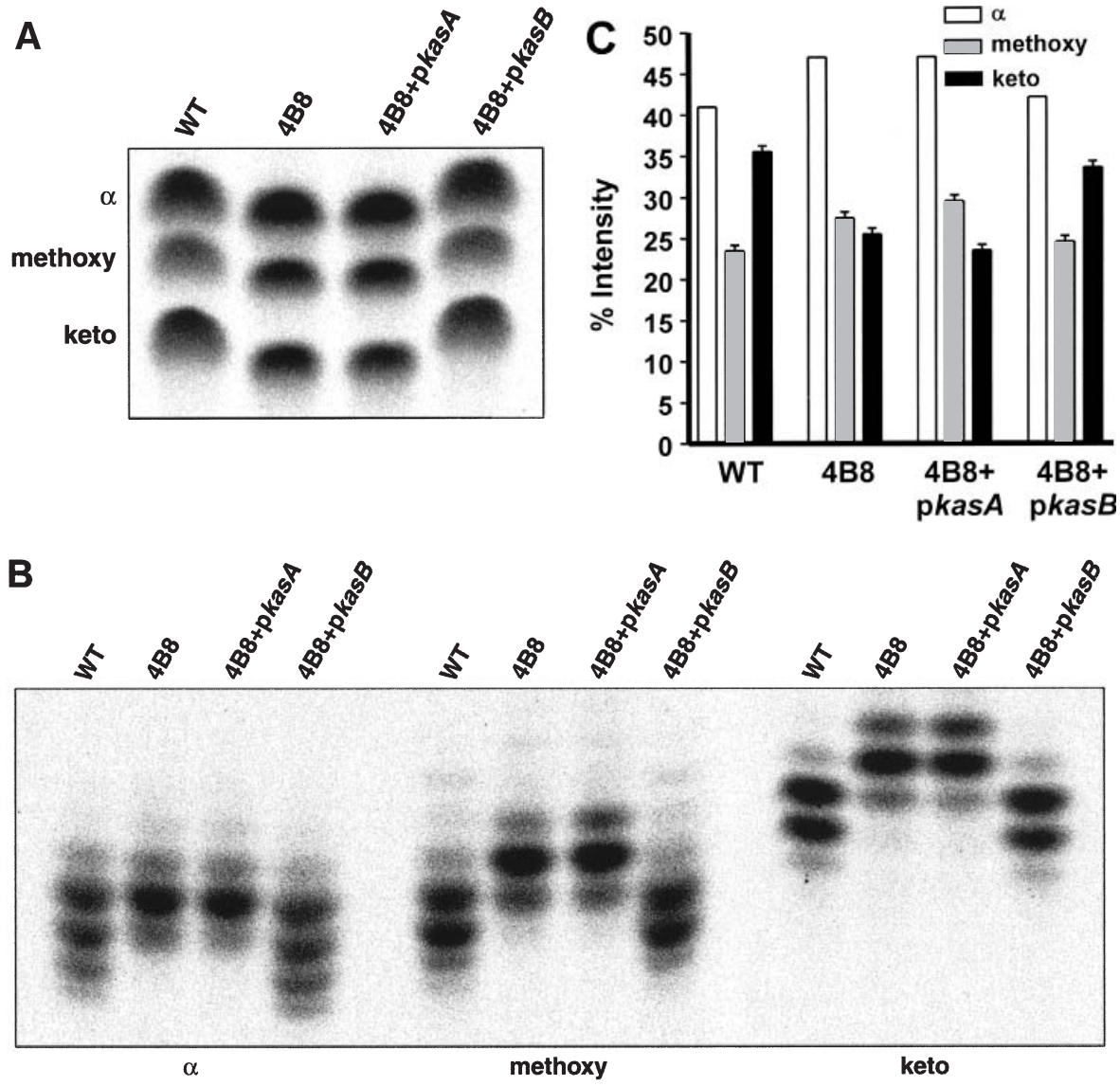

Fig. 4. A and B. Mycolate profiles of *M. marinum* labelled with ^{14}C-acetate as revealed by silica and reverse phase HPTLC respectively. C. Relative intensity of a mycolate type compared to the total mycolates.

mainly 24 carbons ($m_4 = 21$, Fig. 6A). Therefore, the 2–4 carbon unit lacking in the mutant mycolates is in the mero-chains. The location of the shortening in the mero-chains can be determined by oxidative cleavage of mycolates, provided that the substances contain ethylenic bonds that are converted by permanganate into dihydroxylated compounds, which in turn are oxidized by periodate to yield long-chain fatty acids and dicarboxylic acids (van Rudloff, 1956). Accordingly, this reaction was applied to purified oxygenated mycolates of wild type and *kasB* mutant of *M. marinum,* which are most exclusively ethylenic substances, and the resulting fatty acids were esterified by diazomethane and purified. Analysis of the MALDI-TOF mass spectra of the monoesters derived from the mycolates of *M. marinum* showed no difference between the products from wild type and *kasB* mutants (data not shown), indicating that the 2–4 carbon unit difference is not located in the distal portion of the mycolates. This conclusion was supported further by analysis of the GC-MS spectra of the monoesters derived from the oxygenated mycolates of *M. marinum*, which allowed the definitive location of the keto and methoxy groups in the *trans* ethylenic methoxy- and keto-mycolates ($m_1 = 15,17$; $m_2 = 13,15$; Fig. 6A). On the other hand, MALDI-TOF mass spectra of the hydroxylated diesters clearly revealed size differences between oxygenated mycolates isolated from wild type and the *kasB* mutant (Fig. 6B and C). As pyrolysis showed that α-branches of all types of *M. mari-*

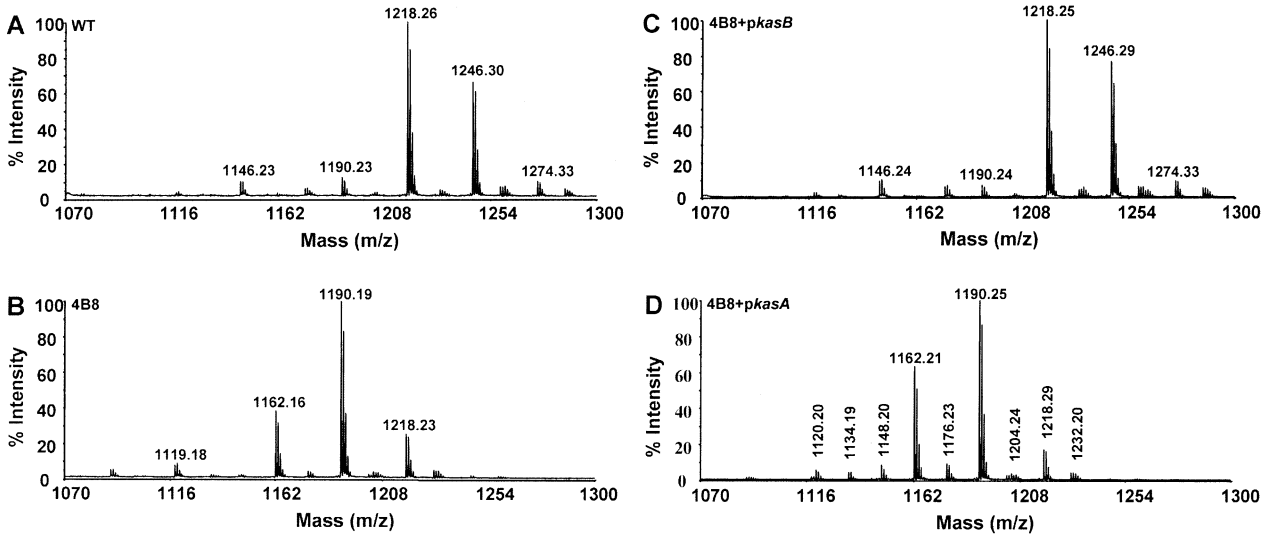

Fig. 5. MALDI-TOF mass spectra of the keto-MAMEs of *M. marinum* strains. Values indicated the masses of the sodium adducts (M + 23).

num mycolates had the same size ($m_4 = 21$), it was deduced that m_3 were 17 or 19 for wild type, but 13 or 15 for the mutant (Fig. 6A–C). Together, these data showed that the 2–4 carbon units lacking in the oxygenated mycolates of the *kasB* mutants are located in the proximal portion of the mero-chains.

KasB-*dependent mycolate elongation is essential for cording and cell wall impermeability*

A correlation between cording in culture and virulence has long been recognized for *M. tuberculosis* H37Rv and H37Ra strains (Middlebrook *et al*., 1947), and a change of morphology from granular, dry, and rough to viscous, moist, and smooth was observed by Calmette and Guerin during their serial passage of *Mycobacterium bovis* to create the BCG vaccine strain (Guerin, 1957). Recently, *M. tuberculosis* cording has been shown to require cyclopropanation of α-mycolates (Glickman *et al*., 2000). Wild-type *M. marinum* also forms cords in liquid culture (Fig. 7A) and shows a rough colony morphology on agar (Fig. 7E). In contrast, the 4B8 mutant showed strikingly altered morphology that appeared as non-ordered small aggregates in liquid (Fig. 7B) and smooth colonies on agar (Fig. 7F). The cording and colony morphology abnormalities of the mutant were completely

Table 1. MALDI-TOF MS data of the MAMEs of *M. marinum* strains.

MA type	Mm strain	Total carbon number of free acids												
		73	74	75	76	77	78	79	80	81	82	83	84	85
α	WT	1104	***1118***	1132	***1146***		1174		1202					
	4B8	1104	***1118***		1146									
	4B8 + p*kasB*		***1118***	1132	***1146***	1160	***1174***		1202					
	4B8 + p*kasA*	1104	***1118***		1146									
M	WT							1206	1220	***1234***		***1262***		1290
	4B8					1178		***1206***		1234				
	4B8 + p*kasB*							1206	1220	***1234***	1248	***1262***		1290
	4B8 + p*kasA*					***1178***		***1206***						
K	WT								***1218***		***1246***			
	4B8				1162		***1190***		1218					
	4B8 + p*kasB*								***1218***		***1246***			
	4B8 + p*kasA*				***1162***		***1190***		1218					

The pseudomolecular mass values $[M + Na]^+$ of the major homologues are represented in italics and bold. Only molecular species representing >20% of the mixture are indicated. MA, mycolic acid; M, methoxy; K, keto; Mm, *M. marinum*.

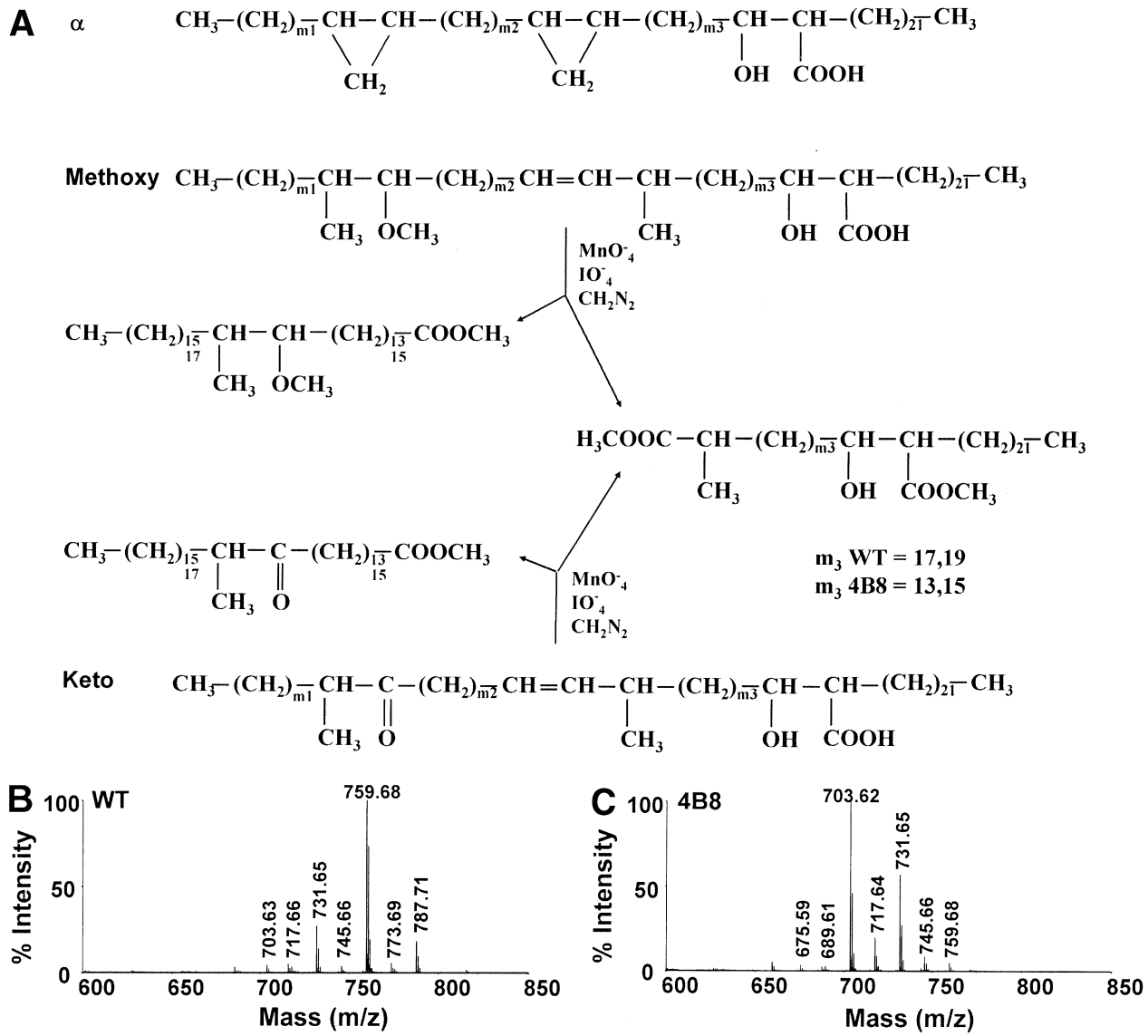

Fig. 6. A. Structures of the major species of α-, methoxy- and keto-mycolates of *M. marinum* and illustration of the strategies for determining m_1 to m_4 of purified methoxy- and keto-mycolates that contain a double bond, which can be cleaved by a permanganate/periodate reaction into analysable products.
B and C. MALDI-TOF MS of the hydroxylated diesters of *M. marinum* wild type and the 4B8 mutant respectively.

recovered by expressing *M. tuberculosis kasB* (Fig. 7C and G), but not *kasA* (Fig. 7D and H). Expression of *kasA* actually made the mutant grow slower on agar (Fig. 7H), similar to its slow growth rate in liquid (Fig. 3A). As *M. marinum* wild type and the *kasB* mutants elaborated similar amounts of cell wall lipids and the trehalose mycolates, it follows that *kasB*-dependent elongation of mycolates is a second important factor for cording. The cording and colony morphology abnormalities of the 4B8 mutant did not, however, affect the ultrastructure of the mutant cell envelope, as assessed by electron microscopy (data not shown).

Given the importance of mycolates in maintaining cell wall integrity, we examined cell wall permeability for *M. marinum* wild type and the *kasB* mutants. As shown in Fig. 8A, whereas wild type and the *kasB*-complemented mutant were resistant to SDS at 0.01–0.5%, the 4B8 mutant (with or without *kasA* complementation) showed extreme sensitivity. As a second test of cell wall integrity, we examined the ability of *M. marinum* strains to resist loss of lipophilic stain, a well-known 'acid fast' characteristic of mycobacterial cell walls, presumed to depend on mycolates. As shown in Fig. 8B, the 4B8 mutant was much more vulnerable to

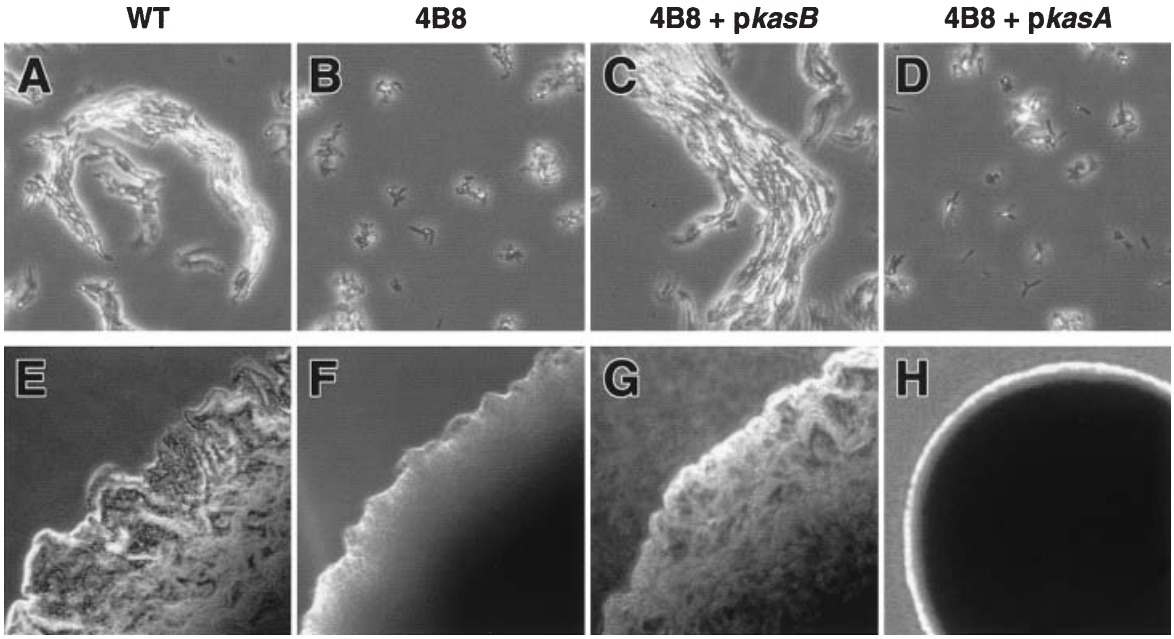

Fig. 7. A–D. Cording of *M. marinum* in 7H9 broth.
E–H. Colony morphology of *M. marinum* on 7H10 agar grown to 7 days (E, F and G) or 10 days (H). Colony size of 4B8 + p*kasA* at 7 days (image not shown) was ~10-times smaller than wild type.

destain than wild type or the *kasB*-complemented mutant.

To measure cell wall permeability directly, we examined diffusion of the lipophilic compound, [^{14}C]-chenodeoxycholate, into *M. marinum*. As predicted, the 4B8 mutant accumulated this compound at a much higher initial rate (~ threefold in the first 6 min) than wild type or the *kasB*-complemented mutant (Fig. 8C). Collectively, these results demonstrate that *kasB*-mediated elongation of mycolates (or the secondary effect on accumulation of keto-mycolates) is essential for normal mycobacterial cell wall barrier function.

KasB-*dependent cell wall impermeability is essential for antibiotic resistance*

To determine whether *kasB*–dependent cell wall barrier is essential for antibiotic resistance, we tested sensitivity of *M. marinum* strains to several antibiotics with different properties. As shown in Table 2, the 4B8 mutant was much more sensitive than wild type to lipophilic antibiotics such as rifampin (RIF), ciprofloxacin (CIP) and erythromycin (ERY), exhibiting 12- to 60-fold lower MIC (minimal inhibitory concentration), as tested by the agar method. In contrast, no differences were detected between wild type and the mutant in resistance to hydrophilic antibiotics such as INH and streptomycin (STR). Resistance to lipophilic antibiotics was fully restored for the 4B8 mutant by expressing *M. tuberculosis kasB*, but not *kasA* (Table 2). Activity of these lipophilic antibiotics has been shown to depend on the rate of penetration across mycobacterial cell wall (Brennan and Nikaido, 1995; Liu and Nikaido, 1999). The correlation between diffusion of ^{14}C-chenodeoxycholate and sensitivity to lipophilic antibiotics strongly suggests that *kasB*-dependent cell wall impermeability is essential for mycobacterial resistance to these antibiotics.

Cerulenin synergizes with RIF activity

Cerulenin (CER), a well-characterized potent inhibitor for KAS of both the FAS-I and FAS-II systems, has been shown to inhibit KasA and KasB activity *in vitro* and to affect mycolate biosynthesis (Kremer *et al*., 2000; 2002; Schaeffer *et al*., 2001). No differences in MIC (0.2 μg ml^{-1}) for CER were detected between wild type and the 4B8 mutant (Table 2). To determine whether there was synergy between CER and RIF, we treated wild-type *M. marinum* with a subinhibitory concentration of CER

Table 2. Minimal inhibitory concentration (MIC) (μg ml^{-1}) of *M. marinum* strains for different antibiotics tested by the agar method.

Strains	RIF	CIP	ERY	INH	STR	CER
WT	0.2	0.06	30	30	8	0.2
4B8	0.01	0.005	0.5	30	8	0.2
4B8 + p*kasB*	0.2	0.06	30	30	8	0.2
4B8 + p*kasA*	0.01	0.005	0.5	30	8	0.2

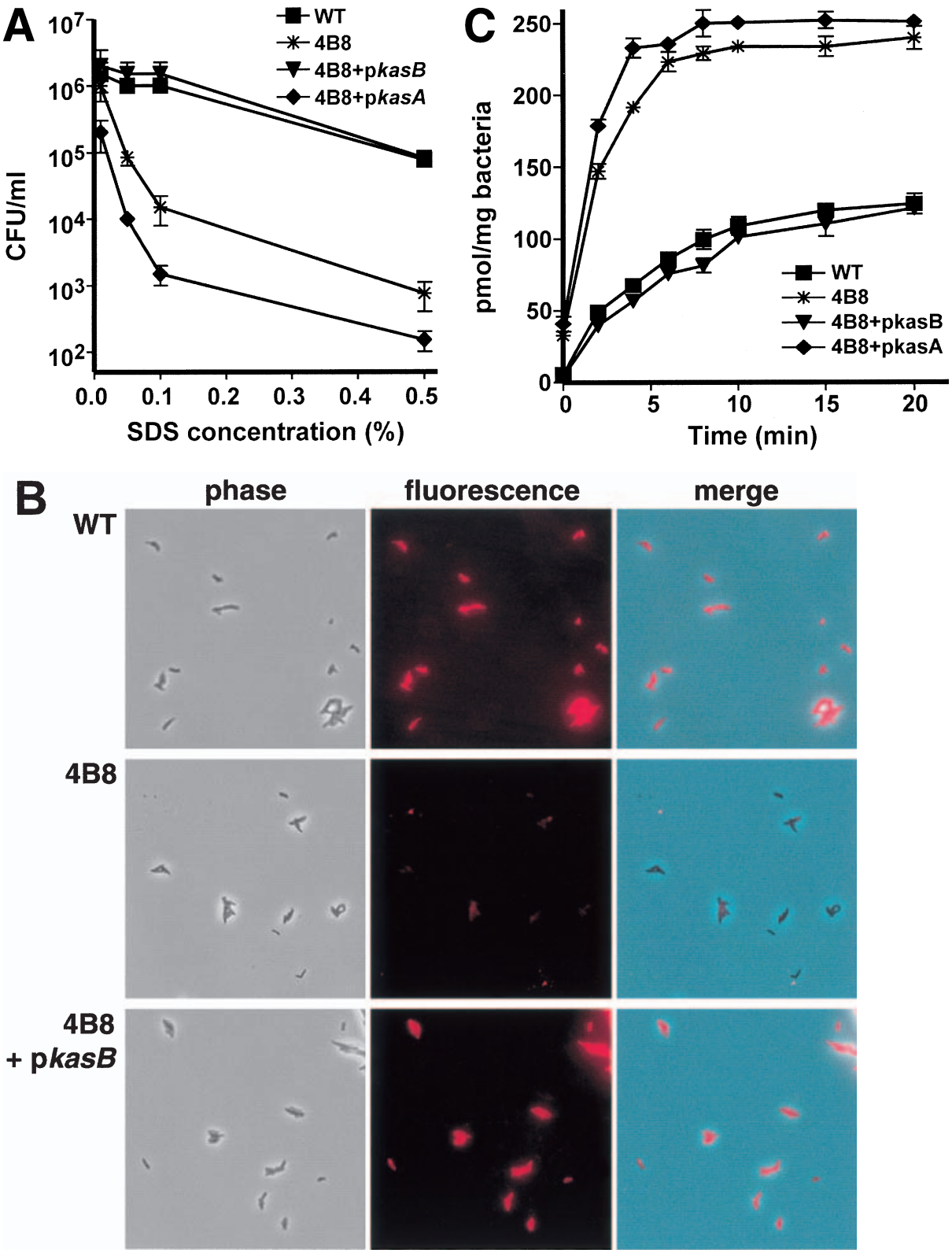

Fig. 8. Measurement of *M. marinum* cell wall permeability.
A. Sensitivity of *M. marinum* to SDS.
B. Resistance of *M. marinum* cell wall to acid destain following three destain procedures.
C. Kinetic of accumulation of [^{14}C]-chenodeoxycholate by *M. marinum*.

(0.1 μg ml^{-1}) together with varying concentrations of RIF and examined MIC by the broth culture method. As shown in Fig. 9, presence of CER significantly increased susceptibility of wild type to RIF, from an MIC of 0.3 μg ml^{-1} (no CER) to 0.04 μg ml^{-1}, close to MIC (0.02 μg ml^{-1}) for the 4B8 mutant (Fig. 9). In contrast, there was no synergy between CER and STR (data not shown), a hydrophilic antibiotic that presumably enters mycobacteria by a different route.

KasB *is essential for resistance to macrophage antimicrobial activity*

We examined whether *kasB* is required for cell wall integrity of intracellular *M. marinum* in macrophages by acid-fast staining. As shown in Fig. 10A, intracellular wild type and the *kasB*-complemented mutant were more resistant to destain than the 4B8 mutant. To determine whether this cell wall defect could increase sensitivity of intracellular *M. marinum* to host defence molecules that might be encountered inside a phagosome or phagolysosome (Kisich *et al*., 2002; Duits *et al*., 2003), we compared susceptibility of *M. marinum* strains to the human neutrophil defensin peptide 1 (HNP-1) and the synthetic defensin-like compound protamine. The 4B8 mutant was significantly more sensitive than wild type to both HNP-1 (Fig. 10B) and protamine (data not shown). In addition, the 4B8 mutant was extremely susceptible to lysozyme at concentrations that had minimal effect on wild type (Fig. 10C). The sensitivity of the mutant to HNP-1, protamine, and lysozyme was completely reverted to wild type by expressing *M. tuberculosis kasB* (Fig. 10B and C, and data not shown). To determine whether the *in vitro* susceptibility of the *kasB* mutants to these antimicrobial molecules is relevant to the *in vivo* macrophage antimycobacterial activity, we examined maturation of the *M. marinum*-containing phagosome of MDM infected by wild type and the *kasB* mutants. Like *M. tuberculosis*, wild-type *M. marinum* inhibits fusion of the bacteria-containing phagosome with lysosomes, so that the bacteria can replicate within a vacuole protected from a variety of host defence molecules (Barker *et al*., 1997; Russell, 2001). As shown in Fig. 11A–D, the vast majority of the wild-type *M. marinum* bacteria (>95%) did not co-localize with the lysosomes, which were visualized with the tracer Lysotracker Red, which fluoresces only at acidic pH. In contrast, 30–40% of the *kasB* mutant bacteria co-localized with lysosomes, as indicated by overlap of the bacteria-containing phagosomes and the Lysotracker-labelled acidic compartments. The loss of inhibition of phagosome-lysosome fusion by the *M. marinum kasB* mutant was fully complemented by expressing *M. tuberculosis kasB (*data not shown). Together, these results suggest that *kasB*-dependent effects on cell wall mycolates are required for mycobacterial resistance to macrophage defence mechanisms.

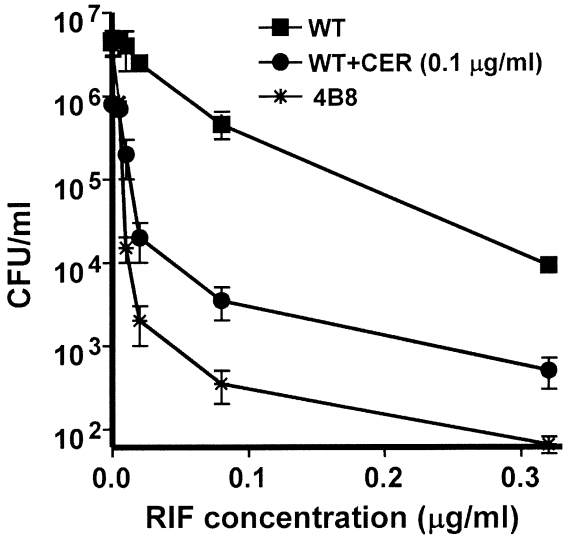

Fig. 9. Synergy between CER and RIF. *M. marinum* wild type or the 4B8 mutant was cultured in 7H9 broth in the presence or absence of CER (0.1 μg ml^{-1}) together with RIF (0.005, 0.01, 0.02, 0.08, 0.32 μg ml^{-1}) or in the absence and MIC was examined by the broth culture method.

Discussion

In this work, we have analysed the role of *kasB* in mycolate biosynthesis in *M. marinum* and shown by HPTLC and MALDI-TOF MS that *kasB* is required for full elongation of each of the three types of mycolates by ~2–4 carbon units. Detailed analyses by argentation TLC, infrared spectroscopy, MALDI-TOF MS, NMR and chemical degradation experiments showed that this *kasB*-mediated extension occurs in the proximal portion of the mero-chain of the mycolates (i.e. the end nearest to the arabinogalactan-peptidoglycan complex). In addition to their defect in mycolate chain length, the *kasB* mutants showed altered ratios among the three types of mycolates, with a significant reduction of keto-mycolates that was accompanied by a compensatory increase of α- and methoxy-mycolates. A current model for the structure of the mycobacterial cell wall suggests that the α-branches and mero-chains of mycolic acid residues align parallel to each other and perpendicular to the plane of the cell surface (Brennan and Nikaido, 1995; Barry *et al*., 1998; Daffe and Draper, 1998; Jarlier and Nikaido, 1994), with covalent linkage of mycolates to the arabinogalactan-peptidoglycan complex. We propose that the 2–4-carbon extension at the proximal portions of the mero-chains is necessary for the distal portions of the mero-chains to play their architectural role in the cell wall. An alternative, but not mutually exclusive, possibility is that distribution of

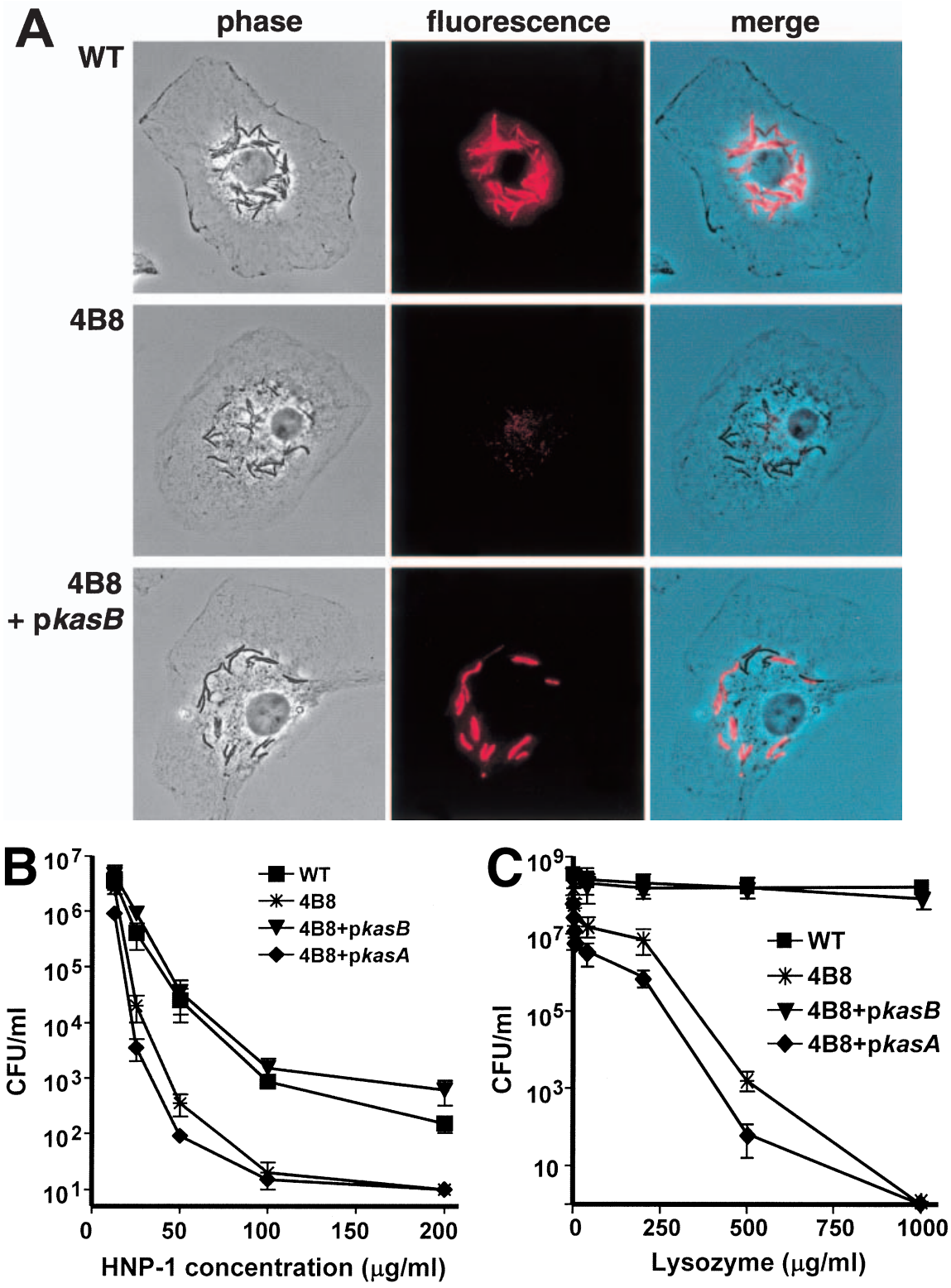

Fig. 10. A. Resistance of intracellular *M. marinum* in MDM (24 h post infection) to acid destain.
B and C. Susceptibility of *M. marinum* to HNP-1 and lysozyme respectively.

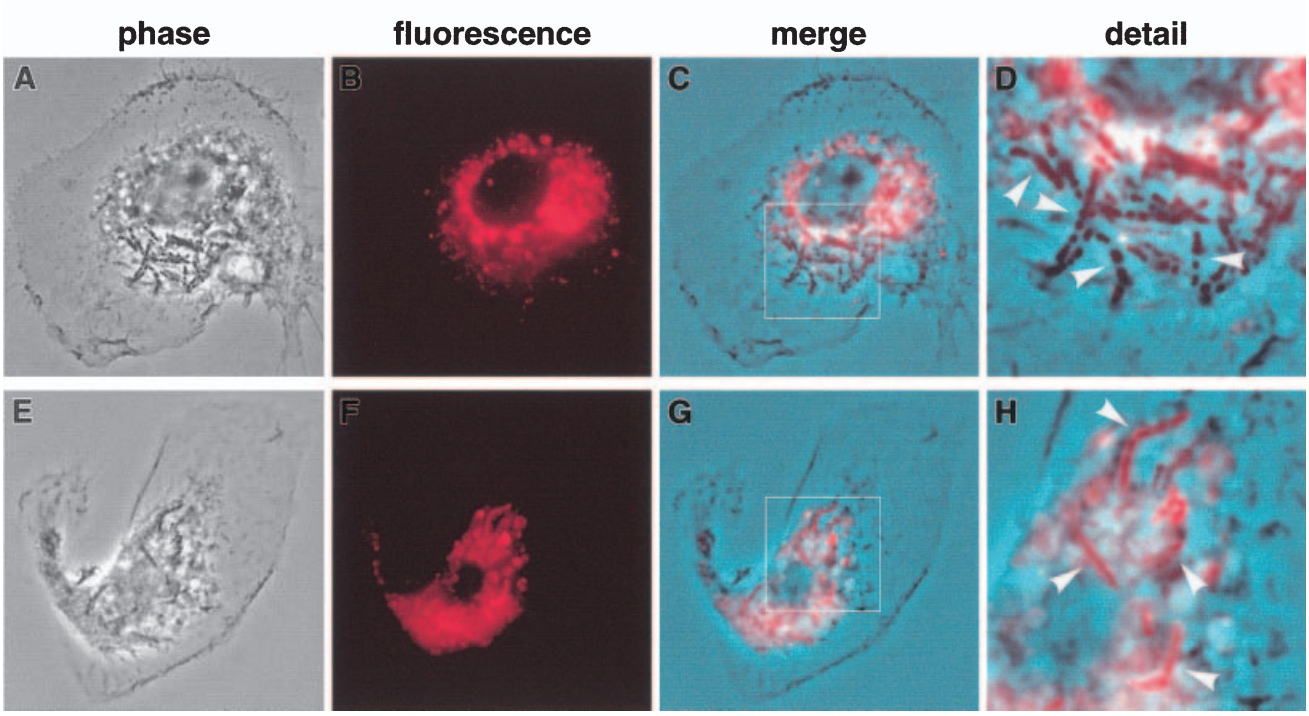

Fig. 11. Inhibition of phagosome maturation by *M. marinum*. MDMs were infected by wild type (A–D) or the 4B8 mutant (E–H) at an MOI of 3. At 24 h post infection, MDMs were incubated with fluorescent Lysotracker Red for labelling of acidic lysosomal compartments. Fusion of *M. marinum*-containing phagosomes with lysosomes is indicated by overlap of the entire bacteria with the red fluorescence, as this demonstrates that the phagosome is at low pH (approximately pH 5.5). Several bacteria (D, wild type; H, 4B8) are indicated by arrowheads. D and H are enlarged sections of C and G, respectively, to better illustrate co-localization of *kasB* mutant bacteria with lysosomes (H) and lack of co-localization for wild type (D).

the three types of mycolates on the cell wall at proper ratios is required for maintaining proper cell wall integrity. In any case, these small changes in mycolate length and composition must have a major effect on organization of the bacterial permeability barrier. We are currently investigating these possibilities for the permeability defect in the absence of *kasB*.

Our results are consistent with the hypothesis that *kasA* is involved in initial extension of the FAS-II-mediated growth of the mycolate chains, and *kasB* is involved primarily in extension to full lengths (Kremer *et al.*, 2000; Slayden and Barry, 2002). It is, however, somewhat surprising that the mycolates in the *M. marinum kasB* mutant are only 2–4 carbons shorter than wild type. Based on *in vitro* assays of KAS enzyme activity in *M. smegmatis* cell lysates, it has been proposed that *kasB* may be required for addition of ~14 carbons to the intermediate mycolate products to reach the final full-lengths (Slayden and Barry, 2002). It is, of course, possible that there is some redundancy in function between *kasA* and *kasB*, so that either enzyme is capable of adding carbons to the growing chain *in vivo*, but *kasB* is more efficient in the *in vitro* assay for chains of 40 or more carbons. However, it is clear that there is not total functional redundancy of the two enzymes *in vivo*, both because absence of *kasB* leads to specific shortening of the mero-chains by 2–4 carbons and because extra-chromosomal addition of *kasB*, but not *kasA*, can fix this defect. Thus, the last 2–4 carbon additions require *kasB* specifically, and not simply an increase in total FAS-II KAS activity.

Given the minimal effects of *kasB* disruption on mycolate length and composition and undetectable effects on other cell wall lipids and cell envelope ultrastructure, the extent of the changes in cell wall permeability in the *kasB* mutants is unexpected. The *kasB* mutants exhibited a ~threefold higher diffusion rate than wild type for the hydrophobic compound chenodeoxycholate to cross the cell wall, and this increased permeability made the mutant bacteria significantly more susceptible to lipophilic antibiotics, defensins and lysozyme. It is intriguing to speculate about the why these small changes of mycolate composition cause such major disruption of the overall physiology of the cell wall. One hypothesis is that appropriate packing of the mycolates covalently associated with the cell wall is essential to restriction of cell wall fluidity, as suggested by Liu and Nikaido (1999) while examining a *M. smegmatis* mutant that was blocked in the synthesis of mature mycolic acids. Changes in mycolate length or composition might significantly affect packing, resulting in increased fluidity and ultimately permeability of the cell wall. We

have found that the *kasB* mutants exhibit much higher sensitivity than wild type to growth arrest at elevated temperatures (34–35°C, unpubl.), which is consistent with this hypothesis. Direct tests for mycobacterial cell wall fluidity have been performed using differential scanning calorimetry (Liu and Nikaido, 1999), and assay of the *kasB* mutant in comparison to wild type by this method should provide a direct test of this hypothesis.

The increased susceptibility of the *kasB* mutants to lipophilic antibiotics suggests that pharmacological inhibition of *kasB* could be extremely useful in therapeutic regimens in synergy with traditional lipophilic antibiotics such as RIF. As an initial approach to this clinically important problem, we showed that interference with KAS activity by a subinhibitory concentration of CER markedly synergized with the bactericidal activity of RIF for wild-type *M. marinum*. We suggest that this is a proof in principle of the therapeutic potential of *kasB* inhibition. *M. marinum* and *M. tuberculosis* are sufficiently genetically related that it is very likely that our findings are relevant to the treatment of tuberculosis. In this context, it is interesting to note that several derivatives of thiolactomycin (TLM, a potent and more specific inhibitor of KasA and KasB than CER) have recently been found to be more potent inhibitors of KasB than TLM itself (Kremer *et al*., 2000). Therefore, more extensive structure-activity studies of derivatives of these compounds, together with a better understanding of KasB catalysis, could lead to discovery of more potent and specific inhibitors for KasB with therapeutic potential. Because our work demonstrates that these studies can be done using the *M. tuberculosis kasB* gene to complement the *kasB* mutant of *M. marinum*, it is possible that novel antibiotic discovery could be carried out in an intact pathogenic organism capable of infecting macrophages and ectotherms, but with minimal risk to investigators.

Finally, this work has demonstrated that *kasB* is required for full virulence of *M. marinum* in macrophage infection. Likely, this is a result of the extreme sensitivity of the *kasB* mutants to innate antimicrobial mechanisms within macrophages, such as defensins and lysozyme. Defensins are potent antimicrobial peptides present in a variety of cell types including neutrophils and macrophages (Risso, 2000; Duits *et al*., 2002), and accumulation of defensins on the bacterial cell surface has been observed for *M. tuberculosis* inside the phagosomes of both macrophages and neutrophils (Kisich *et al*., 2002). Although the phagosome containing wild-type *M. tuberculosis* (Russell, 2001) or *M. marinum* (Barker *et al*., 1997) does not fuse efficiently with lysosomes, the *M. marinum kasB* mutant is inefficient at maintaining this block in phagosome maturation. Loss of *kasB* may result in damage of *M. marinum* by low concentrations of host defence molecules in the early phagosome or reduced ability for *M. marinum* to inhibit phagosome-lysosome fusion. In either case, the *kasB* mutant bacteria end up in a compartment in which they are exposed to higher concentrations of host defence molecules to which they are significantly more susceptible. We believe that these studies reinforce the utility of the *M. marinum* model of mycobacterial pathogenesis and of the M^4 technique for creating, identifying, and studying mycobacterial genes required for survival of this important and complex pathogen family in their eukaryotic hosts.

Experimental procedures

Bacterial strains and media

Mycobacterium marinum strain M and the DH5α strain of *Escherichia coli* were cultured as described (Gao *et al*., 2003).

Isolation of M. marinum *mutants with transposon insertions in the* kasB *gene*

A *M. marinum* mutant library was generated by the M^4 procedure exactly as previously described (Gao *et al*., 2003). Briefly, a *mariner*-based transposon mutagenesis plasmid was electroporated into log-phase *M. marinum*, and bacteria in which transposition occurred were identified by sequential selections on kanamycin (Kan)- and sucrose-containing plates. Kan- and sucrose-resistant colonies were repeatedly subcloned to insure that each colony arose from a single transposon insertion, and ~1000 individual mutants were screened for defective intracellular growth in J774 cells (ATCC TIB67) and bone marrow-derived macrophages (MDMs) using our previously described method (Gao *et al*., 2003). A total of 24 mutants were isolated that exhibited more than fivefold reduction of CFUs for intracellular bacteria as compared to wild type after 4 days of infection. Recovery and sequencing of the transposon insertion sites were performed as described (Gao *et al*., 2003). Sequencing was performed by the Biomolecular Resource Center at the University of California, San Francisco. Similarity searches were performed using BLASTP and BLASTN at the NCBI site (http://www.ncbi.nlm.nih.gov/BLAST) and the incomplete *M. marinum* genome data base at the Sanger Center site (http://www.sanger.ac.uk/Projects/M_marinum/).

Complementation of M. marinum kasB *mutants*

To complement the *M. marinum kasB* mutants by *M. tuberculosis kasB* gene, the coding sequence of *M. tuberculosis kasB* (Cole *et al*., 1998) was amplified by polymerase chain reaction (PCR) using primers Rv2246kasBU1 (5′-GGGTAC CACCACTTGCGGGGGCGAGTC-3′) and Rv2246kasBD1 (5′ GGCCCAAGCTTCCTGTCGCGTAACGC-3′) (Invitrogen) and cloned into pLYG206.Zeo, similarly as we previously described (Gao *et al*., 2003). pLGY206.Zeo was constructed by replacing the Kan-resistant gene (Kan^r) (*Hpa*I-*Spe*I fragment) of pMV261.Kan with the Zeocin-resistant gene (Zeo^r) (*Eco*RV-*Xba*I fragment) derived from pEM7.Zeo (Invitrogen). The vector pLYG206.Zeo alone or containing cloned genes

was transformed into *M. marinum* strains by electroporation under optimal conditions as previously described (Gao *et al*., 2003). The PCR primers for *M. tuberculosis kasA* were Rv2245kasAU2 (5′-CCAGTCAGCCTTCCACCGCTAATG GCGG-3′) and Rv2245kasAD2 (5′-GGCAAGCTTCGTGCT TCAGTAACGCCCGAAG-3′). The primers for *M. tuberculosis accD6* were Rv2247accD6U2 (5′-CTACAATCATGGC CCCCGAGGCGGTTGGC-3′) and Rv2247accD6D2 (5′-CCGAAGCTTGCTCGCGGTCAGAACTACAGCG-3′). The primers for *M. marinum kasA* were MmkasAU1 (5′-TGAC CAAGCCTTCCACTGCTAATGGCGGTTACCC-3′) and MmkasAD1 (5′-CGCAAGCTTTTAGTAGCGCCCGAAAGC GAGCGC-3′). Expression of the cloned genes was detected by SDS-PAGE of whole-cell lysates, which showed accumulation of proteins of predicted sizes.

Extraction and analyses of cell wall lipids

Extraction and separation of *M. marinum* cell wall lipids to polar lipids (PL), apolar lipids (AL), and mycolic acid methyl esters (MAMEs) were performed as described (Besra, 1998). Polar lipids and AL were resolved in one or two dimensions by high performance TLC (HPTLC) plates (EM Science) on either silica or reverse phase surface, yet no differences were detected between wild type and the *kasB* mutants. MAMEs were first separated to α-, methoxy- and keto-mycolates on silica HPTLC plates by hexanes:ethyl acetate (95:5, v/v), and the purified fractions from preparative plates were further resolved on reverse phase HPTLC plates by chloroform:methanol (40:60, v/v). Lipids were visualized by spraying with 20% sulphuric acid in ethanol and charring. For metabolic labelling of cell wall lipids, *M. marinum* were incubated with [^{14}C]-acetic acid (1 μCi ml^{-1}) for 2 h and the cell wall lipids were isolated and separated, exposed to a Cyclone phosphor screen, and analysed by the Cyclone Phosphor System software (Packard Instrument Company).

Argentation TLC analysis

To search for the presence of ethylenic compounds, purified mycolate fractions were resolved on $AgNO_3$-impregnated silica HPTLC plates developed with CH_2Cl_2 or petroleum ether/diethylether (9:1, v/v, three runs).

Oxidative degradation of mycolates

Cleavage of double bonds in oxygenated mycolates was performed by permanganate-periodate oxidation (van Rudloff, 1956) at 30°C in tertiary butanol as solvent for 16 h. The reaction was stopped by addition of potassium pyrosulphite (Fluka) until decolorization of the solution. After acidification, the oxidative products were extracted with ether, washed with distilled water, and dried. The products were methylated using diazomethane and purified for further analyses.

NMR analysis

^{1}H-NMR spectra of purified MAMEs were obtained in $CDCl_3$ (100% D) using a Bruker AMX-500 spectrometer at 298 K. Chemical shifts values (in p.p.m.) were relative to the internal $CHCl_3$ resonance (at 7.27 p.p.m.).

MALDI-TOF MS analysis

MALDI-TOF mass spectra in the positive mode were acquired on a Voyager-DE STR mass spectrometer (PerSeptive Biosystems, Framingham, MA) equipped with a pulsed nitrogen laser emitting at 337 nm. Samples were analysed in the Reflectron mode using an extraction delay time of 100 ns and an accelerating voltage of 20 kV. To improve the signal-to-noise ratio, 150 single shots were averaged for each spectrum and four individual spectra were accumulated to generate a summed spectrum. Calibration mixture 1 (SequazymeTM Peptide Mass Standards Kit, Perseptive Biosystems) was used to calibrate the spectra. Internal mass calibration was performed with sodiated synthetic corynomycolate ($[C_{32}H_{\cdot 64}O_{\cdot 3} + Na]^+$) and its methyl ester derivative ($[C_{33}H_{\cdot 66}O_{\cdot 3} + Na]^+$) or with sodiated MAME ($C_{76}H_{\cdot 148}O_{\cdot 3}$, $[M + Na]^+$) (Laval *et al*., 2001). Mycolates dissolved in chloroform (1 mM) was applied as droplets of 1 μl, followed by 0.5 μl of the matrix solution [2,5-dihydroxybenzoic acid (10 mg ml^{-1}) in $CHCl_3$/CH_3OH (1:1, v/v)].

Infrared spectroscopy analysis

IR spectra of samples as films on NaCl discs were recorded using a Perkin-Elmer FTIR 1600 spectrometer.

Gas chromatography

Fatty acid methyl esters (FAMEs) derived from saponification of *M. marinum* were analysed by gas chromatography (GC) on a Hewlett-Packard 5890 series II apparatus equipped with an OV1 capillary column (0.30 mm × 25 m) using helium gas. The temperature program involved an increase from 100 to 300°C (5°C min^{-1}), followed by 10 min at 300°C. The temperature of the injection port used was 250°C, except of the analysis of purified α-, methoxy- and keto-mycolates in which a temperature of 350°C was used to allow the pyrolysis of mycolates and the identification of their α-branched chain. GC-MS analyses of FAMEs, purified mycolates and their oxidative products in the electron impact mode were performed on a HP 5889X mass spectrometer (electron energy, 70 eV) coupled to a HP 5890 series II gas chromatograph fitted with a column identical to that used for GC.

Measurement of cording and cell wall permeability

Cording or colony morphology of *M. marinum* was observed after growth in 7H9 broth or on 7H10 agar. Resistance to SDS was assayed by inoculating *M. marinum* (10^4 ml^{-1}) in 7H9 broth containing SDS (0.01, 0.05, 0.1, or 0.5%, v/v), culturing for 4 days at 30°C, and enumeration of CFUs on 7H10 agar. Acid-fast stain and destain were performed using a TB fluorescent stain kit T (Difco). For *in vitro*-grown *M. marinum*, liquid culture at mid-log phase was centrifuged at 50 *g* for 5 min to remove large aggregates. The suspension was spread onto a microscope glass slide, dried, stained with

the Auramine-Rhodamine T solution, destained with Decolorizer TM repetitively for 2 min in each time, and observed using a fluorescent microscope. For intracellular *M. marinum* in MDMs, the stain and destain procedure was similarly performed at 24 h after infection. Diffusion of [^{14}C]-chenodeoxycholate (PerkinElmer) into *M. marinum* was measured as described (Jackson *et al.*, 1999), with an incubation time of 0, 2, 4, 6, 8, 10, 15 or 20 min.

Susceptibility of M. marinum *to antibiotics*

Susceptibility of *M. marinum* to antibiotics was determined either on 7H10 agar or in 7H9 broth. For testing on agar, a suspension of single bacteria was spotted on 7H10 (10^2/spot) containing antibiotics at different concentrations, and the MIC was determined as the minimal concentration of an antibiotic that completely inhibited appearance of colonies on agar. For testing in broth culture, a suspension of single bacteria was inoculated to 7H9 (10^4 ml^{-1}) containing antibiotics at different concentration and cultured for 4 days before enumeration of CFUs on 7H10. The MIC for tests in broth cultures was determined as the minimal concentration of an antibiotic that completely inhibited increase of CFUs.

Susceptibility of M. marinum *to defensins and lysozyme*

To examine susceptibility of *M. marinum* to human neutrophil defensin peptide-1 (HNP-1) or protamine, a suspension of single bacteria was inoculated to 7H9 (10^4 ml^{-1}) containing either peptide at different concentrations and cultured for 4 days before enumeration of CFUs on 7H10. Susceptibility to lysozyme was similarly tested, except that 10^6 bacteria ml^{-1} were inoculated because of the extreme susceptibility for the *kasB* mutants.

Inhibition of phagosome maturation by M. marinum

Bone marrow-derived macrophages infected by *M. marinum* (MOI = 3) for 24 h were incubated with Lysotracker Red (Molecular Probes) at 100 nM for 40 min. Then, the monolayer was washed twice to remove residual Lysotracker Red and further incubated for 1 h before imaging.

Acknowledgements

The authors thank Robert Chalkley and A. L. Burlingame for assistance with lipid analysis and Luisa M. Stamm and M. A. Lanéelle for critical reading of the manuscript. This work was supported by grants from the NIH to E.J.B. and J.S.C. L.Y.G. is supported by T32 AI07334.

References

Barker, L.P., George, K.M., Falkow, S., and Small, P.L. (1997) Differential trafficking of live and dead *Mycobacterium marinum* organisms in macrophages. *Infect Immun* **65:** 1497–1504.

Barry, C.E., Lee, R.E., Mdluli, K., Sampson, A.E., Schroeder, B.G., Slayden, R.A., and Yuan, Y. (1998) Mycolic acids: structure, biosynthesis and physiological functions. *Prog Lipid Res* **37:** 143–179.

Besra, G.S. (1998) Preparation of cell-wall fractions from *Mycobacteria*. In *Mycobacteria Protocols.* Parish, T., and Stoker, N.G. (eds). New Jersey: Humana Press, pp. 91–107.

Brennan, P.J., and Nikaido, H. (1995) The envelope of mycobacteria. *Annu Rev Biochem* **64:** 29–63.

Chemlal, K., Huys, G., Laval, F., Vincent, V., Savage, C., Gutierrez, C. *et al.* (2002) Characterization of an unusual *Mycobacterium*: a possible missing link between *Mycobacterium marinum* and *Mycobacterium ulcerans*. *J Clin Microbiol* **40:** 2370–2380.

Cole, S.T., Brosch, R., Parkhill, J., Garnier, T., Churcher, C., Harris, D., *et al.* (1998) Deciphering the biology of *Mycobacterium tuberculosis* from the complete genome sequence. *Nature* **393:** 537–544.

Daffe, M., Laneelle, M.A., and Lacave, C. (1991) Structure and stereochemistry of mycolic acids of *Mycobacterium marinum* and *Mycobacterium ulcerans*. *Res Microbiol* **142:** 397–403.

Daffe, M., and Draper, P. (1998) The envelope layers of mycobacteria with reference to their pathogenicity. *Adv Microb Physiol* **39:** 131–203.

Davidson, L.A., Draper, P., and Minnikin, D.E. (1982) Studies on the mycolic acids from the walls of *Mycobacterium microti*. *J Gen Microbiol* **128:** 823–828.

Dolin, P.J., Raviglione, M.C., and Kochi, A. (1994) Global tuberculosis incidence and mortality during 1990–2000. *Bull World Health Organ* **72:** 213–220.

Dubnau, E., Chan, J., Raynaud, C., Mohan, V.P., Laneelle, M.A., Yu, K., *et al.* (2000) Oxygenated mycolic acids are necessary for virulence of *Mycobacterium tuberculosis*. mice. *Mol Microbiol* **36:** 630–637.

Duits, L.A., Ravensbergen, B., Rademaker, M., Hiemstra, P.S., and Nibbering, P.H. (2002) Expression of beta-defensin 1 and 2 mRNA by human monocytes, macrophages and dendritic cells. *Immunology* **106:** 517–525.

Gao, L.Y., and Kwaik, Y.A. (2000) The modulation of host cell apoptosis by intracellular bacterial pathogens. *Trends Microbiol* **8:** 306–313.

Gao, L.Y., Groger, R., Cox, J.S., Beverley, S.M., Lawson, E., and Brown, E.J. (2003) Transposon mutagenesis of *Mycobacterium marinum* identifies a locus linking pigmentation and intracellular survival. *Infect Immun* **71:** 922–929.

George, K.M., Yuan, Y., Sherman, D.R., and Barry, C.E. (1995) The biosynthesis of cyclopropanated mycolic acids in *Mycobacterium tuberculosis*. Identification and functional analysis of CMAS-2. *J Biol Chem* **270:** 27292–27298.

Glickman, M.S., Cox, J.S., and Jacobs, W.R.J. (2000) A novel mycolic acid cyclopropane synthetase is required for cording, persistence, and virulence of *Mycobacterium tuberculosis*. *Mol Cell* **5:** 717–727.

Glickman, M.S., Cahill, S.M., and Jacobs, W.R.J. (2001) The *Mycobacterium tuberculosis* cmaA2 gene encodes a mycolic acid trans-cyclopropane synthetase. *J Biol Chem* **276:** 2228–2233.

Guerin, C. (1957) In *The History of BCG*. Rosenthal, S.R. (ed). London: J. & A. Churchill, pp. 48–57.

Jackson, M., Raynaud, C., Laneelle, M.A., Guilhot, C., Laurent-Winter, C., Ensergueix, D., *et al.* (1999) Inactivation of the antigen 85C gene profoundly affects the mycolate content and alters the permeability of the *Mycobacterium tuberculosis* cell envelope. *Mol Microbiol* **31:** 1573–1587.

Jarlier, V., and Nikaido, H. (1994) Mycobacterial cell wall: structure and role in natural resistance to antibiotics. *FEMS Microbiol Lett* **123:** 11–18.

Kisich, K.O., Higgins, M., Diamond, G., and Heifets, L. (2002) Tumor necrosis factor alpha stimulates killing of *Mycobacterium tuberculosis* by human neutrophils. *Infect Immun* **70:** 4591–4599.

Kremer, L., Douglas, J.D., Baulard, A.R., Morehouse, C., Guy, M.R., Alland, D., *et al.* (2000) Thiolactomycin and related analogues as novel anti-mycobacterial agents targeting KasA and KasB condensing enzymes in *Mycobacterium tuberculosis*. *J Biol Chem* **275:** 16857–16864.

Kremer, L., Dover, L.G., Carrere, S., Nampoothiri, K.M., Lesjean, S., Brown, A.K., *et al.* (2002) Mycolic acid biosynthesis and enzymic characterization of the beta-ketoacyl-ACP synthase A-condensing enzyme from *Mycobacterium tuberculosis*. *Biochem J* **364:** 423–430.

Laval, F., Laneelle, M.A., Deon, C., Monsarrat, B., and Daffe, M. (2001) Accurate molecular mass determination of mycolic acids by MALDI-TOF mass spectrometry. *Anal Chem* **73:** 4537–4544.

Liu, J., and Nikaido, H. (1999) A mutant of *Mycobacterium smegmatis* defective in the biosynthesis of mycolic acids accumulates meromycolates. *Proc Natl Acad Sci USA* **96:** 4011–4016.

Mdluli, K., Slayden, R.A., Zhu, Y., Ramaswamy, S., Pan, X., Mead, D., *et al.* (1998) Inhibition of a *Mycobacterium tuberculosis* beta-ketoacyl ACP synthase by isoniazid. *Science* **280:** 1607–1610.

Middlebrook, G., Dobos, R.J., and Pierce, C. (1947) Virulence and morphological characteristics of mammalian tubercle bacilli. *J Exp Med* **86:** 175–184.

Qureshi, N., Takayama, K., and Schnoes, H.K. (1980) Purification of C30–56 fatty acids from *Mycobacterium tuberculosis* H37Ra. *J Biol Chem* **255:** 182–189.

Ramakrishnan, L., Valdivia, R.H., McKerrow, J.H., and Falkow, S. (1997) *Mycobacterium marinum* causes both long-term subclinical infection and acute disease in the leopard frog (*Rana pipiens*). *Infect Immun* **65:** 767–773.

Ramakrishnan, L., Federspiel, N.A., and Falkow, S. (2000) Granuloma-specific expression of *Mycobacterium* virulence proteins from the glycine-rich PE-PGRS family. *Science* **288:** 1436–1439.

Risso, A. (2000) Leukocyte antimicrobial peptides: multifunctional effector molecules of innate immunity. *J Leukoc Biol* **68:** 785–792.

van Rudloff, E. (1956) Periodate-permanganate oxidations. V. Oxidation of lipids in media containing organic solvents. *Can J Chem* **34:** 1414–1418.

Russell, D.G. (2001) *Mycobacterium tuberculosis*: here today, and here tomorrow. *Nat Rev Mol Cell Biol* **2:** 569–577.

Schaeffer, M.L., Agnihotri, G., Volker, C., Kallender, H., Brennan, P.J., and Lonsdale, J.T. (2001) Purification and biochemical characterization of the *Mycobacterium tuberculosis* beta-ketoacyl-acyl carrier protein synthases KasA and KasB. *J Biol Chem* **276:** 47029–47037.

Slayden, R.A., and Barry, C.E. (2002) The role of KasA and KasB in the biosynthesis of meromycolic acids and isoniazid resistance in *Mycobacterium tuberculosis*. *Tuberculosis* **82:** 149–160.

Talaat, A.M., Reimschuessel, R., Wasserman, S.S., and Trucksis, M. (1998) Goldfish, *Carassius auratus*, a novel animal model for the study of *Mycobacterium marinum* pathogenesis. *Infect Immun* **66:** 2938–2942.

Tonjum, T., Welty, D.B., Jantzen, E., and Small, P.L. (1998) Differentiation of *Mycobacterium ulcerans*, *M. marinum*, and *M. haemophilum*: mapping of their relationships to *M. tuberculosis* by fatty acid profile analysis, DNA-DNA hybridization, and 16S rRNA gene sequence analysis. *J Clin Microbiol* **36:** 918–925.

Yuan, Y., Lee, R.E., Besra, G.S., Belisle, J.T., and Barry, C.E. (1995) Identification of a gene involved in the biosynthesis of cyclopropanated mycolic acids in *Mycobacterium tuberculosis*. *Proc Natl Acad Sci USA* **92:** 6630–6634.

Yuan, Y., Zhu, Y., Crane, D.D., and Barry, C.E. (1998) The effect of oxygenated mycolic acid composition on cell wall function and macrophage growth in *Mycobacterium tuberculosis*. *Mol Microbiol* **29:** 1449–1458.